Atmosphere-Ocean
Publication details, including instructions for authors and subscription information:
http://www.tandfonline.com/loi/tato20

Seasonal and interannual variability in the circulation of Puget Sound, Washington: A box model study

A. L. Babson [a] , M. Kawase [b] & P. MacCready [b]
[a] School of Oceanography , University of Washington , Seattle, WA, 98195-5351, USA E-mail:
[b] School of Oceanography , University of Washington , Seattle, WA, 98195-5351, USA
Published online: 21 Nov 2010.

To cite this article: A. L. Babson , M. Kawase & P. MacCready (2006) Seasonal and interannual variability in the circulation of Puget Sound, Washington: A box model study, Atmosphere-Ocean, 44:1, 29-45, DOI: 10.3137/ao.440103

To link to this article: http://dx.doi.org/10.3137/ao.440103

Seasonal and Interannual Variability in the Circulation of Puget Sound, Washington: A Box Model Study

A. L. Babson*, M. Kawase and P. MacCready

School of Oceanography, University of Washington
Seattle, WA 98195-5351 USA

[Original manuscript received 30 August 2004; in revised form 7 June 2005]

ABSTRACT *A prognostic, time-dependent box model of circulation in Puget Sound, Washington is used to study seasonal and interannual variations in residence times and interbasin transports. The model is capable of reproducing salinity variability in the Sound at seasonal timescales, and is shown to have hindcast skill at interannual timescales. Modelled transports vary as much between years as between seasons. The largest seasonal feature is a sharp transport drop in late autumn into the deep Main Basin of the Sound, which is shown to be caused by increased river flow into Whidbey Basin. The high degree of transport variability leads to large interannual differences in residence times; for instance, for Whidbey Basin the residence time varies from 33 to 44 days in the period between 1992 and 2001 and for southern Hood Canal it varies from 64 to 121 days. This indicates that residence time estimates based on a year or less of data may not yield representative values. A forcing sensitivity study shows that in all basins except the South Sound, salinity variability in the Strait of Juan de Fuca accounts for more of the seasonal variability than river variability does. However, year-to-year variability in river discharge affects interannual variability in transports as much as the Strait of Juan de Fuca salinity does. The model demonstrates poorest skill in the basins most affected by the Strait of Juan de Fuca salinity, indicating that the sparse data available for the Strait may not provide adequate boundary conditions for the model.*

RÉSUMÉ *[Traduit par la rédaction] Nous utilisons un modèle de prévision à boîte, fonction du temps, de la circulation dans le détroit de Puget, dans l'État de Washington, pour étudier les variations saisonnières et interannuelles des temps de séjour et du transport entre bassins. Le modèle peut reproduire la variabilité de la salinité dans le détroit aux échelles saisonnières et on constate qu'il donne des résultats rétrospectifs intéressants aux échelles interannuelles. Les transports modélisés varient autant entre les années qu'entre les saisons. La caractéristique saisonnière la plus importante est une diminution marquée du transport en direction du bassin principal profond du détroit à la fin de l'automne, et nous montrons que cela est causé par un accroissement du débit des rivières dans le bassin Whidbey. Le haut degré de variabilité dans le transport mène à de grandes différences interannuelles dans les temps de séjour. Par exemple, pour le bassin de Whidbey, le temps de séjour varie de 33 à 44 jours au cours de la période de 1992 à 2001 et pour le chenal South Hood, il varie de 64 à 121 jours. Ceci indique que les estimations de temps de séjour basées sur une année ou moins de données peuvent conduire à des valeurs non représentatives. Une étude de sensibilité au forçage montre que dans tous les bassins, à l'exception du détroit South, la variabilité de la salinité dans le détroit de Juan de Fuca explique davantage la variabilité saisonnière que ne le fait la variabilité du débit des rivières. Cependant, la variabilité d'année en année dans le débit des rivières a autant d'influence sur la variabilité interannuelle des transports qu'en a la salinité dans détroit de Juan de Fuca. C'est dans les bassins où l'influence de la salinité du détroit de Juan de Fuca est la plus grande que les résultats du modèle sont les moins bons, ce qui indique que les données éparses disponibles pour le détroit peuvent ne pas fournir des conditions aux limites adéquates pour le modèle.*

1 Introduction

Puget Sound is a partially mixed estuarine fjord in Washington State, and the largest such body of water in the contiguous forty-eight states of the United States (Fig. 1). It consists of a series of interconnected basins separated by sills. The double-silled Admiralty Inlet is the primary outlet to the Strait of Juan de Fuca (SJF) which in turn connects to the Pacific Ocean. There are three major branches of Puget Sound off of Admiralty Inlet. The primary branch consists of the deep Main Basin and the shallower South Sound, the latter consisting of numerous branching inlets and separated from Main Basin by a sill and constriction at the Narrows. The other two branches are Hood Canal to the south-west and Whidbey Basin to the north-east. There is a secondary outlet to the SJF at the northern end of Whidbey Basin: the shallow, extremely narrow Deception Pass.

The mean subtidal circulation of Puget Sound is primarily density driven, forced by the contrast between the fresh water

*Corresponding authors e-mail: babsona@ocean.washington.edu

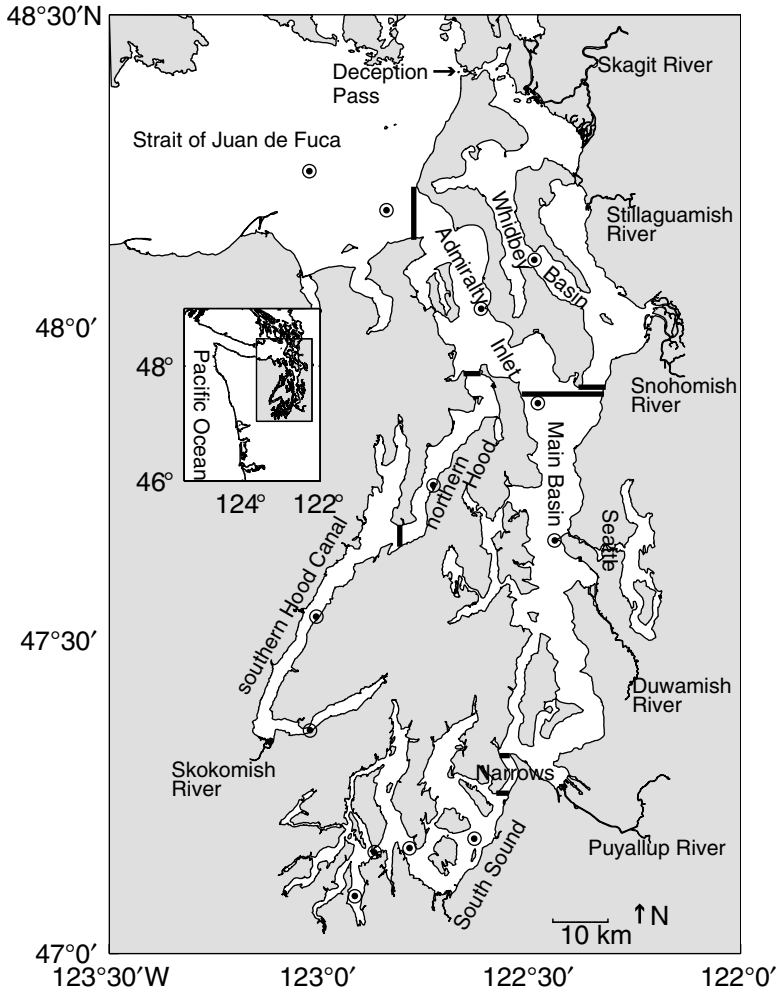

Fig. 1 Map of Puget Sound: bullseyes mark the locations of DoE sampling stations used for calibration, forcing and validation. Thick lines mark model basin boundaries. Major rivers have been labeled, but the model includes twelve others. The inset map shows the relation of the study area to the Pacific Northwest coast.

from rivers and salty marine water at the mouth of Puget Sound. The circulation can be approximated as two-layer exchange flow, with seaward flow at the surface and landward flow at depth. The sill regions have increased vertical mixing, which refluxes part of the fresh surface water landward (Ebbesmeyer and Barnes, 1980).

The Skagit, Stillaguamish and Snohomish rivers entering Whidbey Basin are the largest freshwater input into Puget Sound. The Skagit River alone accounts for more than half of the river flow into Puget Sound (Cannon, 1983). River flow peaks both in winter, due to runoff, and again in late spring or early summer, due to snow melt, and is often at a minimum in September. Other rivers either follow a similar seasonal cycle or have only a single winter peak, if not fed by snow-pack. Upwelling and downwelling off the Washington coast are believed to control the salinity of the water entering the SJF (Barnes and Collias, 1958). The water properties in the SJF outside Admiralty Inlet do not directly reflect those of the Pacific Ocean; it is complicated by SJF bathymetry, which diverts flow northward through the Strait of Georgia, and by mixing with Fraser River water (Holbrook et al., 1980). Seasonally, salinity at the mouth of Admiralty Inlet typically peaks in September, with a lag of several months from the beginning of the coastal upwelling season (Barnes and Collias, 1958; Hickey, 1989). The two forcing functions can reinforce each other, but the relative importance of the two in controlling Puget Sound's circulation is currently unknown. They each exhibit a high degree of interannual variability, in addition to seasonal variability.

Generally speaking, Puget Sound basins are well ventilated and oxygenated. In recent years, however, oxygen depletion has become a greater concern in Hood Canal, where low oxygen events have been associated with fish kills and fishing closures. The long residence time and high productivity here make it susceptible to hypoxia, but it is unclear whether natural variability or eutrophication is the cause of the current problem. Estimates of transport and residence time by basin that include seasonal forcing variability are thus important for both research and management considerations.

A small number of previous studies addressed seasonal and interannual variability of Puget Sound's hydrography and

circulation (Ebbesmeyer et al., 1989). Though the Puget Sound historical data record is extensive (Collias et al., 1974; Cannon and Laird, 1978; Geyer and Cannon, 1982; Bretschneider et al., 1985; Cannon et al., 1990; Edwards et al., 2004), it is spatially and temporally uneven. Since 1989, the Washington State Department of Ecology (DoE) has expanded its monthly monitoring program of stations distributed throughout the Sound to collect depth profiles of physical properties. A major observational program at the junction of Admiralty Inlet, Main Basin and Whidbey Basin was undertaken from July 2000 to August 2001 as part of a King County (Washington) effort to site the outfall of a sewage treatment plant (Ebbesmeyer et al., 2001).

A range of modelling studies of Puget Sound have been carried out to cover some of the data gaps and to investigate the dynamics (Lavelle et al., 1991; Nairn and Kawase, 2002.). A detailed model of circulation, however, requires significant computational resources; running a large number of cases to study sensitivity is, as yet, impractical. A simpler, less computationally expensive model can explore a wide range of scenarios and provide direction on where to focus the efforts of more advanced models. Previous Puget Sound box models include those of Friebertshauser and Duxbury (1972), Hamilton et al. (1985) and Cokelet et al. (1990); the last of which diagnosed mean annual transports between basin and reach zones using observed mean salinities. Time-dependent box models have been developed for other estuaries to estimate seasonal and interannual variability in transports and residence times (for example, Li et al. (1999) for the Strait of Georgia/Strait of Juan de Fuca system; Hagy et al. (2000) for the Patuxent River estuary).

In this paper, a prognostic box model of Puget Sound circulation is developed for a study of seasonal cycle, interbasin differences and interannual variability in residence times and transports, and their sensitivity to variations in forcing. The model is based on conservation of mass and salt, and parametrized advection, mixing and forcing functions. While the work of Li et al. (1999) was the original basis for this model, we did not use their parametrization because it required too many tunable parameters for this type of application. This application has a greater number of basins, uses global parameters and has a more extensive dataset for a more rigorous validation. We have developed a parametrization scheme that has not been previously used as a box model. We were searching for a scheme appropriate to basin averages, which also allowed the individual responses of each basin to be prominent. Its use here is intended not as a test of a new description of estuarine dynamics, but as a means to investigate Puget Sound circulation variability.

Model formulation and data used for calibration and validation are described in Section 2 along with the experimental design. Section 3 focuses on variability and a comparison of the relative importance of river versus salinity forcing on transport.

2 Methods

a *Model Formulation*

The model divides Puget Sound into seven basins: Admiralty Inlet, Whidbey Basin, Main Basin, the Narrows, South Sound, northern Hood Canal and southern Hood Canal (Figs 1 and 2). Basin boundaries were chosen based on the locations of data stations and sills.

Two-layer estuarine circulation is assumed, so each basin is divided into a surface and a deep box, resulting in a total of fourteen boxes. The depth of no motion, where the tidally averaged velocity crosses zero between an outgoing surface layer and an incoming deep layer, determines the thickness of the surface box, which can vary by basin. These were adopted from the box depths of Cokelet et al. (1990), which were in turn based on the depth of no motion from composites of current meter profiles taken between 1947 and 1983 and compiled by Cox et al. (1984). Basin depths, areas and volumes were calculated from the Puget Sound Regional Synthesis Model (PRISM) digitized bathymetric data (King County Department of Natural Resources, 2002). For reference, these values and other model constants are listed in Table 1.

The model estimates salinity for each box and transports between boxes, including vertical mixing of salt and horizontal and vertical advection of water and salt. Transports are defined as positive seaward and upward.

The model equations are based on conservation of mass and salt as well as parametrizations of additional dynamics. Assuming that water is incompressible, conservation of mass yields a conservation of volume equation for each box

$$-\Gamma_{Seaward} \pm \Gamma_{Interface} + \Gamma_{Landward} + \Gamma_{Forcing} = 0 \quad (1)$$

where $\Gamma_{Seaward}$ is the volume flux through the seaward face of the box, $\Gamma_{Landward}$ is the volume flux through the landward face, $\Gamma_{Interface}$ is the volume flux through the vertical interface (the operator in front is positive for surface boxes and negative for deep boxes), and $\Gamma_{Forcing}$ is the river inflow and volume flux from the SJF. Discharges from the largest rivers enter four of the upper boxes, described in Section 2b.

Change in the salinity of each box with time is balanced by a salt flux convergence

$$\frac{dS}{dt} = \frac{-1}{V}\left(\Sigma F_{Adv} + \Sigma F_{Mixing} + \Sigma F_{Forcing}\right) \quad (2)$$

where S is salinity, V is volume and ΣF stands for the divergence of salt flux due to advection, mixing and SJF forcing (river salt flux is zero) respectively. The advective salt fluxes can be calculated from the volume fluxes according to

$$F_{Adv} = \Gamma S \quad (3)$$

where S from the upstream box is used. The series of equations based on Eq. (2) for each box is solved for salinity at the next time step using a first order forward finite difference scheme

$$S(t + \Delta t) = S(t) - \frac{\Delta t}{V} - \left(\Sigma F_{Adv} + \Sigma F_{Forcing} + \Sigma F_{Mixing}\right) \quad (4)$$

where a timestep of $\Delta t = 0.1$ day was used.

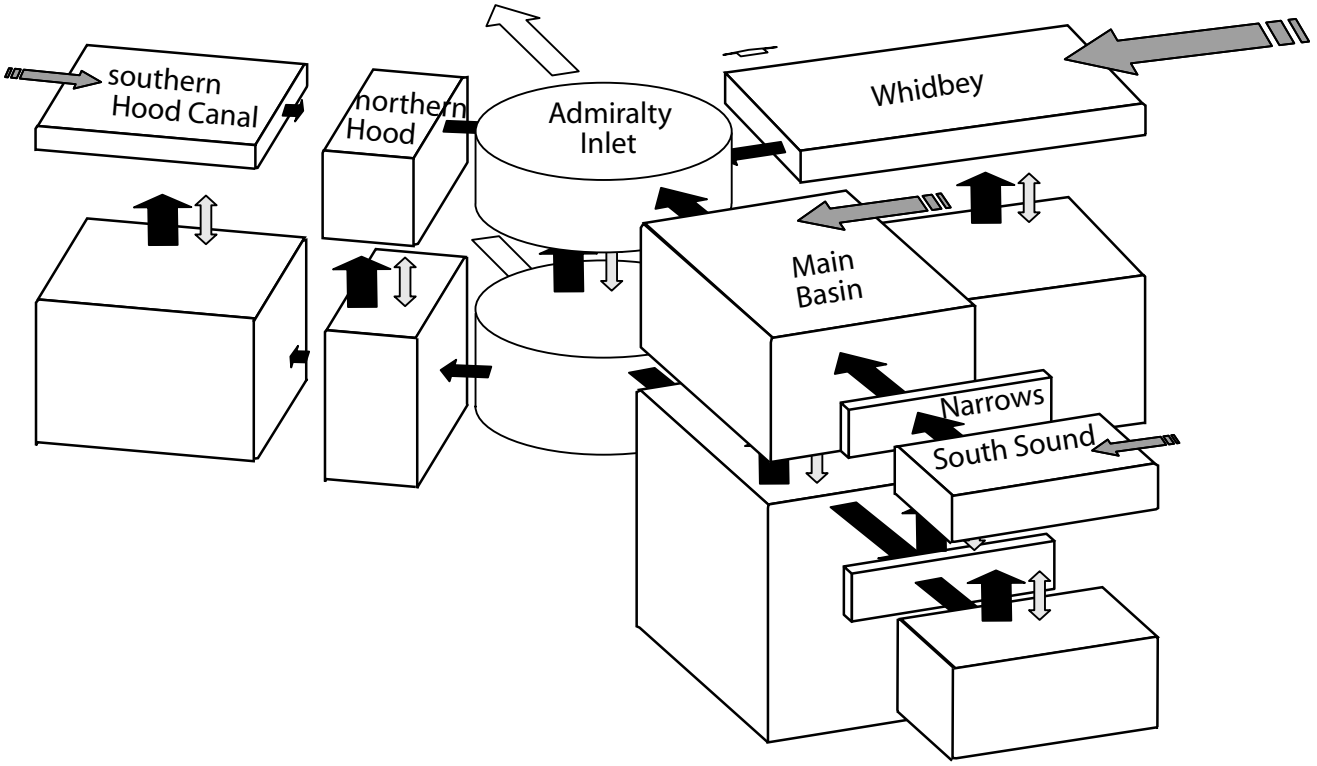

Fig. 2 Model schematic: black arrows represent advection, two-way grey arrows represent mixing, grey arrows with dashed ends represent river inputs and white arrows are outlets to the SJF. Boxes have been scaled to show relative volumes. Arrows have been scaled to transports within each category. Rivers are proportional on a log scale. The Admiralty Inlet mixing arrow is shown at 50%.

TABLE 1. Model constants

	surface box depths (m)	surface volumes 10^{10} (m^3)	deep volumes 10^{10} (m^3)
Admiralty	37.0	1.45	1.96
Main	50.2	2.52	3.96
South Sound	29.9	0.71	0.67
Whidbey	9.1	0.40	2.69
northern Hood	19.8	0.26	0.43
southern Hood	13.0	0.38	1.68
Narrows	21.5	0.04	0.02
definition	symbol	value	units
calibration parameter	α	0.106	–
calibration parameter	λ	0.019	–
calibration parameter	γ	0.2	–
calibration parameter	K_{base}	0.17	$cm^2\ s^{-1}$
acceleration due to gravity	g	9.8	$m\ s^{-2}$
salinity expansion coefficient	β	7.6×10^{-4}	psu^{-1}
drag coefficient	C_D	2.5×10^{-3}	
reference density	ρ_o	1022	$kg\ m^{-3}$

Horizontal volume fluxes are determined from mass conservation and the tidally averaged momentum balance. Classic tidally averaged theories, such as that of Hansen and Rattray (1965), assumed a constant vertical eddy viscosity, determined by fit to observations. In this case both the mid-depth and bottom shear stress were important to slowing the exchange flow. However, using detailed observations in the Hudson River estuary, Geyer et al. (2000) found that the tidally averaged shear stress was dominated by the bottom stress, under stratified conditions. They further found that the tidally averaged exchange flow was reasonably well described by an equation of the form

$$\frac{\Delta u}{\Delta z} = \frac{1}{R}\frac{g}{\rho_o}\frac{h_{deep}}{h_{surf}}\frac{\Delta \rho}{\Delta x} \tag{5}$$

where

$$R = \frac{C_D u_T}{\Delta z}. \tag{6}$$

Here the baroclinic pressure gradient balances tidally averaged bottom stress in the lower layer. The upper layer flow is nearly frictionless, but is constrained by mass conservation. Δu is the difference between top and bottom layer velocities in a basin, Δz is the average layer thickness, $\Delta\rho$ is the horizontal density gradient, ρ_o =1022 kg m^{-3} is the reference density, h is the layer depth and Δx is twice the shortest horizontal

distance between the centre of volume to the boundary of the adjacent box. The subscripts *surf* and *deep* refer to a particular property in the surface or deep boxes. We use a typical value of the drag coefficient, $C_D = 2.5 \times 10^{-3}$, appropriate for depth-averaged flow. u_T is the cross-section-averaged root mean square (r.m.s.) tidal velocity which varies by basin, and is calculated from the results of the Lavelle et al. (1988) tidal model. Since salinity dominates temperature in controlling density in Puget Sound, the depth-averaged horizontal density gradient is calculated as

$$\frac{\Delta\rho}{\Delta x\rho_o} = \frac{(\rho_2 - \rho_1)}{\Delta x\rho_o} = \frac{\beta(S_2 - S_1)}{\Delta x} \tag{7}$$

where $\beta = 7.6 \times 10^{-4}$ psu^{-1} is the salinity expansion coefficient, subscripts 1 and 2 denote depth-weighted properties in seaward and landward basins respectively.

In order to define the u in Eq. (5) in terms of volume fluxes, we use a combination of

$$u = \frac{\Gamma}{A} \tag{8}$$

and a conservation of volume flux for each basin, which is generally of the form

$$u_{surf}A_{surf} + u_{deep}A_{deep} = \Gamma_r \tag{9}$$

where A denotes the cross-sectional area between the boxes and the subscript r refers to river input. The resulting transports have the form

$$\Gamma = -\frac{A_{surf}}{A_{surf+deep}} \times \left[\frac{g\beta(S_2 - S_1)\Delta z h_{deep}A_{deep}}{\Delta x R h_{surf}} + \frac{\Gamma_{landward}A_{landward_{surf+deep}}}{A_{landward_{surf}}} + \Gamma_r\right] \tag{10}$$

with differing numbers of terms depending on the geometry and forcing.

Vertical and deep layer horizontal volume fluxes are determined from mass conservation. In addition to the volume fluxes between the boxes and the transport between Admiralty Inlet and the SJF, flows also exit to the SJF through Deception Pass from the upper Whidbey Basin box. These flows are relatively small compared with those through Admiralty Inlet and are inadequately studied to represent the dynamics correctly. Parametrization of this flow is based on Cokelet et al. (1990) from Knudsen's relations

$$\Gamma_{Dec} = -\frac{\alpha\Gamma_{r_W}S_{Wdeep}}{S_{Wdeep} - S_{Wsurf}} \tag{11}$$

where α is the fraction of river flow exiting through Deception Pass, the subscript *Dec* refers to Deception Pass, and the subscript *W* refers to Whidbey Basin.

Vertical mixing of salt is parametrized as the eddy diffusivity times the vertical salinity difference

$$D = -K_v\frac{\Delta S}{\Delta z}A - K_{base}\frac{\Delta S}{h_{surf}}A \tag{12}$$

where K_{base} is a base level of mixing driven by winds and other processes. The depth of the surface layer is used in the second term instead of Δz because wind mixing is more confined to the surface layer. The parameter K_v is the "effective" eddy diffusivity (Pritchard, 1954; Dyer, 1997), meaning that it is the diffusivity one would apply to the tidally averaged stratification to achieve the tidally averaged vertical turbulent salt flux. While values of K_v have been estimated for many estuaries based on observations (Hansen and Rattray, 1965; Dyer, 1997), there is little guidance in the literature for its parametrization.

Here we construct a parametrization for K_v as a function of $\Delta\rho_v$ (the vertical density difference in a basin) and u_T, based on energy considerations. The instantaneous rate of loss of depth-averaged tidal kinetic energy to bottom friction is given by

$$KE_{loss} = \frac{C_D\rho_o\bar{u}^3}{H} \tag{13}$$

where $\bar{u}$ is the magnitude of the depth-averaged flow and H is the total water depth. The depth-averaged rate of increase of potential energy (*PE*) due to mixing is given by

$$PE_{gain} = \frac{-g}{H}\int_{-H}^{0} K_v\frac{\partial\rho}{\partial z}dz. \tag{14}$$

Lewis (1996) states that, while most of the *PE* gain is physically due to mid-depth shear, PE_{gain} still scales with KE_{loss}, except that one must account for the effect of stratification. Lewis (1996) finds reasonable agreement with observations in the Tees Estuary using a proportionality of the form:

$$\frac{PE_{gain}}{KE_{loss}} = \frac{\alpha_1 R_{iL}}{(1 + \alpha_2 R_{iL})} \tag{15}$$

where R_{iL} is the "layer Richardson number," defined by

$$R_{iL} = \frac{g\Delta\rho' d}{\rho_o(\Delta u')^2} \tag{16}$$

where d is the thickness of the pycnocline, and $\Delta\rho'$ and $\Delta u'$ are the non-tidally averaged versions of $\Delta\rho_v$ and Δu. The functional form of Eq. (15) is based on the early work on

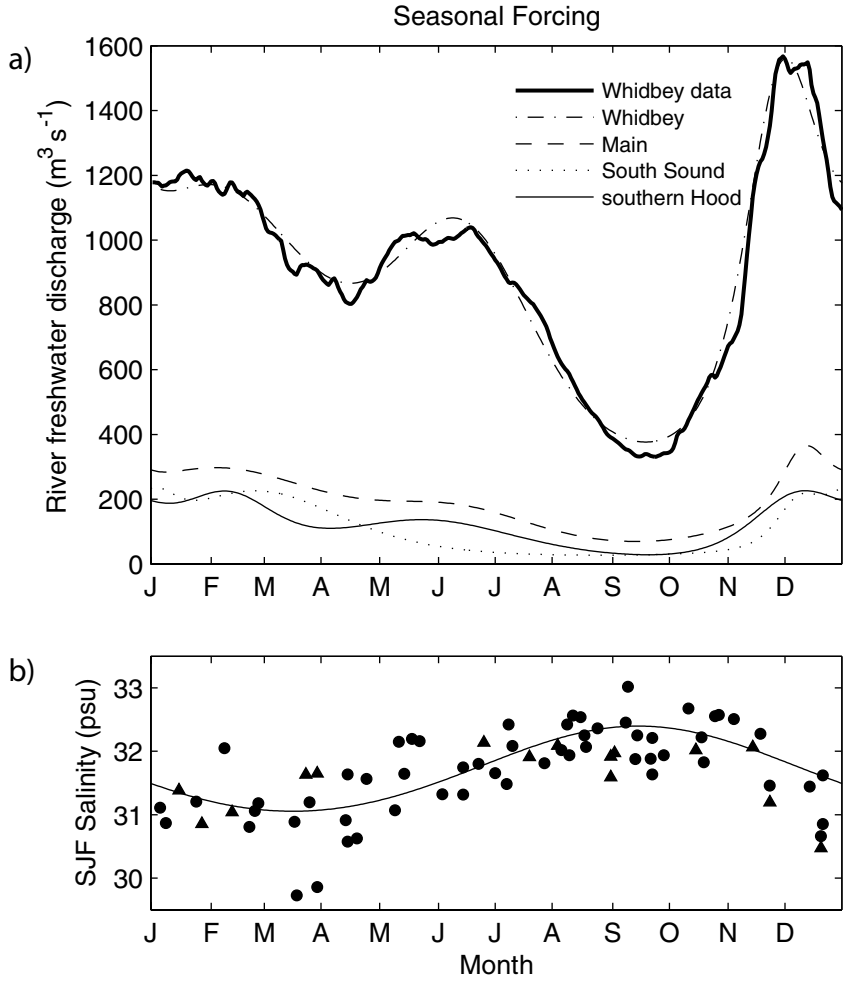

Fig. 3 (a) Idealized composite seasonal river forcing functions entering each basin and an example of the smoothed data for Whidbey Basin to which the function was fit. (b) SJF salinity: the filled circles mark data points from the eastern station and triangles mark data points from the western station (JEMS).

stratified turbulence by Munk and Anderson (1948), and α_1 and α_2 are empirical fitting parameters. We leave these parameters unspecified here, because Lewis' result was for instantaneous mixing rates, whereas our goal is a tidally averaged rate.

Next we assume that the functional form of Eq. (15) still applies to the tidally averaged mixing, and that the tidal averages, denoted by $\langle\ \rangle$, scale as

$$\left\langle PE_{gain}\right\rangle \approx \frac{gK_v\Delta\rho_v}{H} \tag{17}$$

$$\left\langle KE_{loss}\right\rangle \approx \frac{C_D\rho_o {u_T}^3}{H} \tag{18}$$

$$\left\langle R_{iL}\right\rangle \approx \frac{g\Delta\rho_v H}{\rho_o {u_T}^2}. \tag{19}$$

The scaling of $\langle R_{iL}\rangle$ involves the assumption that the r.m.s. shear is proportional to the r.m.s. tidal velocity, which is supported by observations in San Francisco Bay reported by Monismith and Fong (1996). We again convert density differences to salinity differences using Eq. (7), but in this case the gradient is in the vertical, so the difference is between the deep and surface boxes and no weighting is necessary. Using these scalings we may rewrite Eq. (15) to yield an expression for K_v

$$K_v = \frac{\lambda C_D u_T H}{1+\gamma\left\langle R_{iL}\right\rangle} \tag{20}$$

where λ and γ are new empirical fitting parameters to be determined in Section 2c. While the derivation of Eq. (20) is not rigorous, the result is physically reasonable: the effective diffusivity increases with r.m.s. tidal velocity, and decreases as the tidally averaged Richardson number increases.

Horizontal mixing is considered negligible compared with advection and vertical mixing.

b *Forcing*

The model is forced by freshwater inflow from rivers, and by a salinity boundary condition in the SJF, which determines the exchange flow on the seaward faces of the Admiralty Inlet boxes.

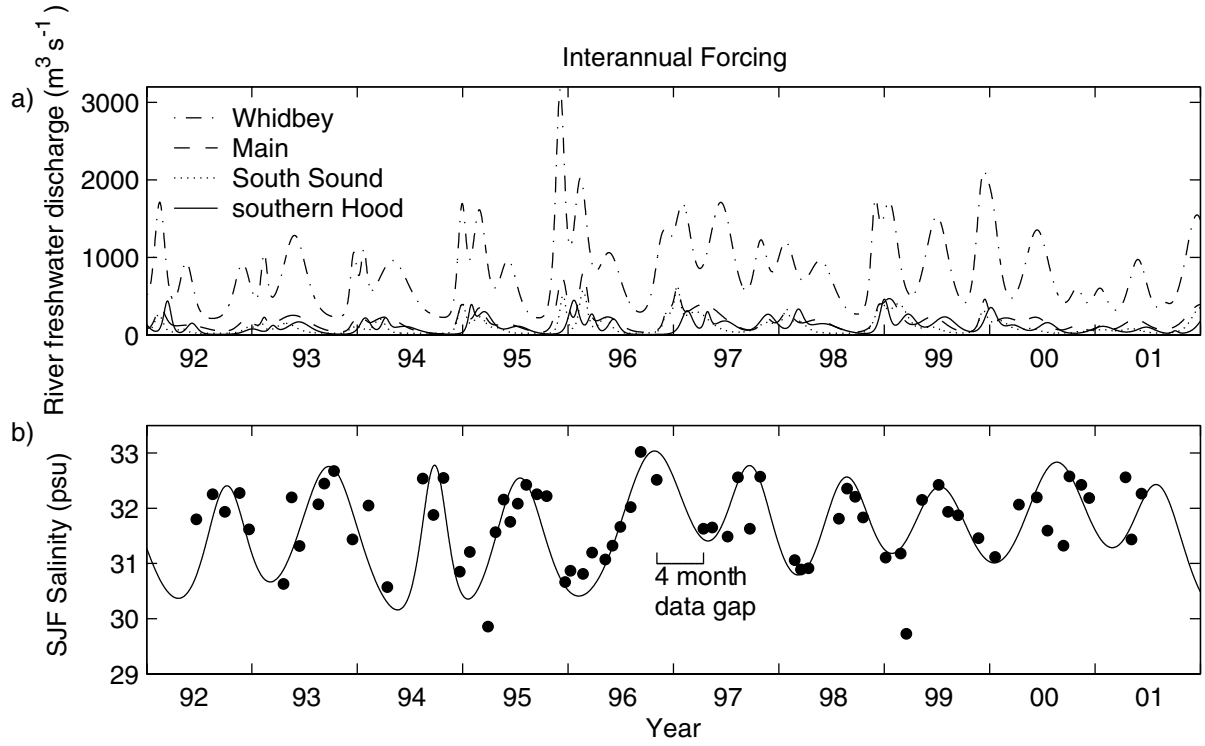

Fig. 4 (a) Interannually varying river forcing and (b) Strait of Juan de Fuca salinity: each has been fit to 1992–2001 data (included for SJF salinity).

The United States Geological Survey (USGS) daily historical river gauge data for many Washington state rivers are available from the early 1900s. The length of the record varies between rivers, and the number of gauged rivers is decreasing. In order to include ungauged rivers and compensate for partially gauged drainage areas, a method developed by Lincoln (1977) is adapted, following Cokelet et al. (1990). A representative gauged reference river is chosen for its hydrographic similarity to the ungauged area; the reference flow is multiplied by the ratio of the gauged to ungauged area. A composite of the seasonal cycle of river flow was constructed by taking the mean flow from 1989–99 for each calendar day. The rivers and proxy rivers entering each basin were summed, and then smoothed using a thirty-day filter. A total of 17 rivers are represented in the model by this method.

The largest rivers (shown as idealized functions in Fig. 3a) enter Whidbey Basin, and have an annual cycle with a large peak in late autumn due to rainfall runoff, a second peak as high flow continues through the winter, and a third peak in early summer due to snowmelt. The rivers flowing into other basins follow this pattern with reduced flow, with the exception of rivers flowing into South Sound which do not have a large snowmelt peak. It is our intent to study the sensitivity of the circulation to the magnitude and timing of each of such hydrological events in future work. In order to facilitate this, idealized functions are fitted to the smoothed river flow data and used as the forcing. Following Li et al. (1999), the peaks in the discharge are represented as hyperbolic secant squared functions

$$\Gamma_r = \Gamma_{r_{base}} + \sum_{n=1}^{3} \Gamma_{r_n} \mathrm{sech}\left(\frac{w_n}{T}\left[t - t_{lag_n} - \frac{T}{2} \right] \right)^2 . \quad (21)$$

Three seasonal peaks for each basin are included. The annual period is T = 365 days. The adjustable river parameters for each peak are: base volume flux, $\Gamma_{r_{base}}$, and amplitude, Γ_{r_n}; width, w_n, and time lag, t_{lag_n}. The parameters in Eq. (21) were adjusted to fit the smoothed river flow data; Fig. 3a includes the smoothed data for Whidbey Basin to show that it is a good fit. For the interannually varying forcing, the same procedure was used, but year-by-year (Fig. 4a).

The SJF salinity was fit to the salinity below 50 m from a DoE station in the eastern SJF occupied quasi-monthly between 1992 and 2001. This station depth is 79 m, which is shallower than most of the SJF. In order to include some deeper data, a 147-m deep Joint Effort to Monitor the Strait (JEMS) station farther west, also sampled quasi-monthly from 1999 to 2001, was included. The SJF salinity function is simplified as a single annual peak following the summer offshore salinity peak due to upwelling. It is defined as

$$S_{SJF} = S_{SJF_{base}} + S_{amp} \mathrm{sech}\left(\frac{w}{T}\left[t - t_{lag} - \frac{T}{2} \right] \right)^2 \quad (22)$$

with the same adjustable parameters as the river flow function, where peak amplitude is now called S_{amp}. The parameters

in Eq. (22) were then adjusted to approximate the data points best and they are shown together in Figs 3b and 4b. In the SJF, the seasonal pattern of the surface salinity follows the deep data with an offset and so was given as deep S_{SJF} − 0.8 psu.

c *Calibration, Validation and Testing Model Skill*

The salinity data used for each box is from eleven of the DoE quasi-monthly monitoring stations occupied between 1989 and 2001 (Fig. 1). This subset of DoE stations was chosen to maximize temporal coverage and to be spatially representative. These observations were made at varying tidal stages that alias higher frequency signals. No corrections have been made for this effect. For three of the basins, single stations were used. The South Sound is the most spatially inhomogeneous, but four stations were available (two for the entire record and two starting in 1996) and their average was used to represent that basin. Averages of two stations each were used in the Main Basin and southern Hood Canal in order to cover data gaps and to be more spatially representative. No data are available for the Narrows so several assumptions were made. Given the high level of mixing here, the level of no motion was set at mid-depth, and the initial salinities were set to the mean of the two adjacent basins. For each basin, data were depth-averaged over surface and deep boxes for comparison with the modelled values.

In order to calibrate the tunable parameters, the model was first forced with steady, long-term mean river flows and SJF salinity. A first order adjustment of λ and γ fit the model salinities to within 1 psu of the annual average of the DoE salinities. Further tuning to reproduce the seasonal cycle of stratification was needed. A composite annual cycle of the data for each box was constructed by averaging the data from an extended time series by year-day into a single representative year. We use the composite in order to overcome the patchiness of the data as well as to produce a representative seasonal cycle. The further adjustment of λ and γ compared the model seasonal salinities with the composite seasonal data for each box within one standard deviation around the monthly averages. K_{base} was also chosen at this stage based on those limits. The only available estimate of Deception Pass transport (Collias et al., 1973) covered the period 19–27 March, so transport during that time was fit to match that estimation by tuning α. While a comparison based on this short time period is not ideal for a flow that is expected to have strong seasonal and interannual variability, we chose it as the simplest option given the data limitation. The resulting parameters are: $\lambda = 0.019$, $\gamma = 0.2$, $K_{base} = 0.17$ cm^2 s^{-1} and $\alpha = 0.106$.

To test model sensitivity to these parameters, a series of runs were carried out where one parameter was varied while the other three were held at their calibrated values. α was varied between 0 and 1, and the other three varied over six orders of magnitude around their calibrated values. We use salinity as the benchmark because that is the property for which we have sufficient data to carry out the calibration. Parameter sensitivity is determined using the criterion that when salinities fall outside of plus or minus one standard deviation of mean salinities with the composite seasonal cycle removed, the parameter value is to be rejected. The resultant bounds on parameter values are then used as bounds for residence time sensitivity.

To validate the model's ability to simulate interannual variations, after being spun up with the composite seasonal cycle, a 10-year validation run with the 1992–2001 forcing sequence was performed. The resulting interannual salinities were compared with the 1992–2001 data sequence. To test the model skill in predicting interannual variability, an ensemble of twenty runs with the forcing years deliberately rearranged in a random order was created. Correlations between the modelled and observed salinities were calculated for the realistic run as well as for each run of the ensemble. A Student-t test was performed, with the null hypothesis being that there is no significant difference in model-data correlation between results with realistic and misordered model forcing. The model's prognostic capabilities are considered valid when the correctly ordered forcing run can capture interannual variations significantly better than the misordered forcing runs.

d *Forcing Sensitivity Experiments*

The model was used to test the relative importance of river forcing versus SJF salinity forcing in driving seasonal and interannual variability. Firstly, to see how each mechanism influences the seasonal cycle, a series of runs was performed, switching each type of forcing between composite seasonal and constant. In order to look at the seasonal anomalies, a run with constant forcing was subtracted from each of the other runs. Secondly, to look at the importance of each forcing mechanism on interannual variability, a series of model runs was carried out varying forcing types between composite seasonal and interannually varying. Thirdly, an all-composite seasonal forcing run was subtracted from the interannually varying runs and each of the mixed forcing runs in order to compare interannual anomalies.

3 Results and discussion

a *Model/Data Comparisons*

The model is able to reproduce the seasonal variability of salinity (Fig. 5), within one standard deviation of the monthly mean most of the time, when forced with functions based on composite seasonal river flow and SJF salinity. The resulting seasonal salinity cycle for all boxes consists of an autumn maximum and a late winter or early spring minimum. There is a distinct seasonal stratification cycle; it is strongest in winter and weakest in autumn. The model captures the interbasin differences in the character of stratification, with the degree and seasonal variation of stratification standing out in Whidbey Basin and southern Hood Canal. However, there are significant discrepancies between the observed and modelled seasonal cycle, such as too much winter stratification in Main Basin and South Sound.

For a quantitative comparison, r^2 values for the correlation between the model salinities and the data are shown in Table 2.

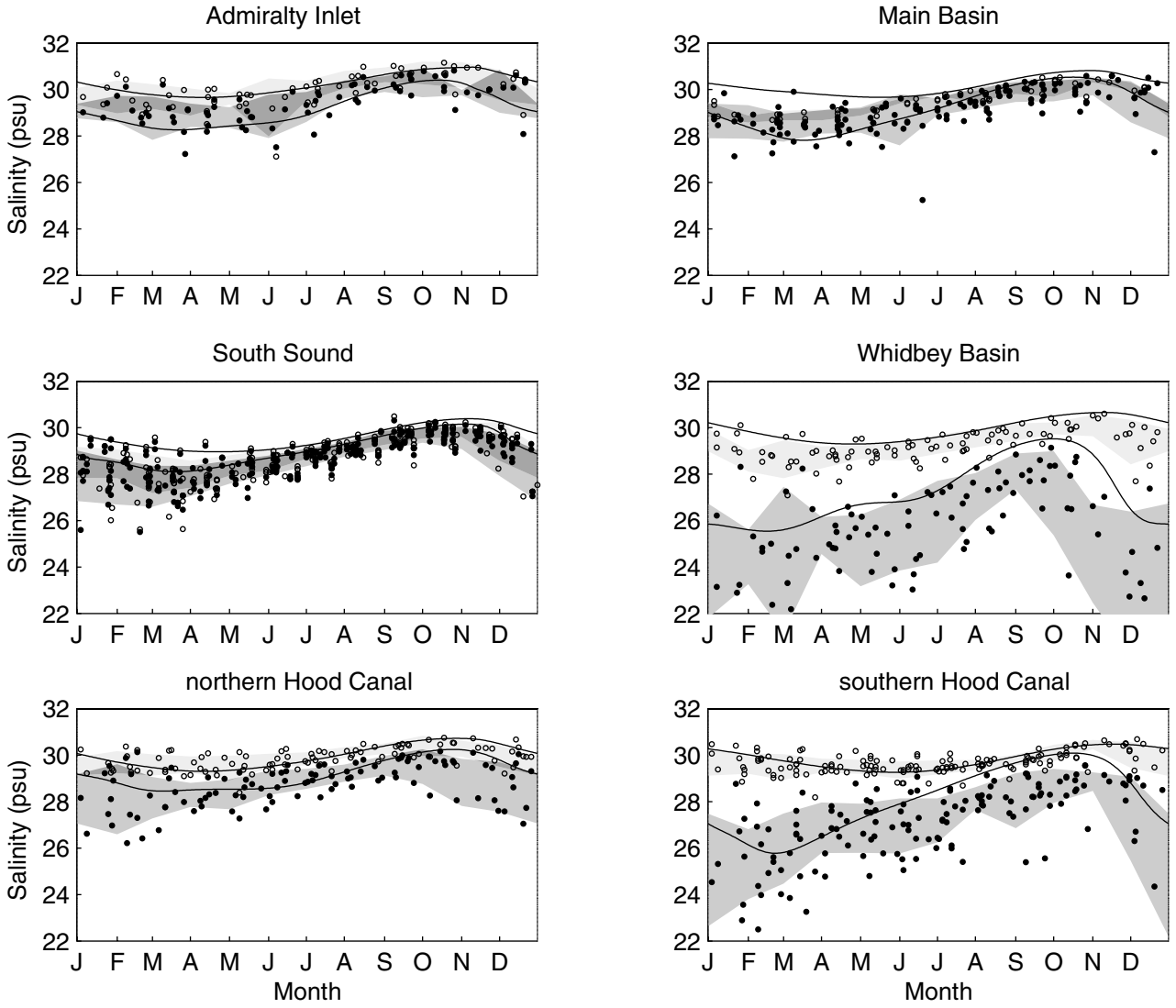

Fig. 5 Comparison between modelled and observed composite seasonal salinity: the lines are the model results. The shaded regions cover the monthly data mean ± one standard deviation; overlaps of the surface and deep regions are in a darker shade of grey. The lines with higher salinity are from the deep boxes, the lines with lower salinities are from the surface boxes. The filled circles are the surface data, the open circles are the deep data.

TABLE 2. r^2 comparison between the modelled and observed salinities.

r^2	composite seasonal	interannual	mean interannual wrong order
Admiralty surface	0.48	0.57	0.24
Admiralty deep	0.43	0.29	0.16
Main surface	0.19	0.62	0.24
Main deep	0.45	0.41	0.17
South Sound surface	0.29	0.71	0.21
South Sound deep	0.41	0.53	0.18
Whidbey surface	0.25	0.52	0.15
Whidbey deep	0.28	0.28	0.17
northern Hood surface	0.28	0.38	0.06
northern Hood deep	0.32	0.36	0.16
southern Hood surface	0.30	0.20	0.11
southern Hood deep	0.28	0.37	0.10

All values in the first two columns are significant at the 95% level. It should be kept in mind that the seasonal run is compared with data that aliases interannual and tidal signals.

When forced with the interannually varying functions (Fig. 4a), the model agreement with data varies by basin and by year. The r^2 agreement improves in most basins in the interannual run, though there are some basins (such as deep Admiralty Inlet) where the correlation deteriorates with interannual forcing; this is likely an effect of the limitations of the salinity boundary condition. A salinity time series produced by Cannon et al. (1990) from a current meter mooring from just outside Admiralty Inlet from December 1983 to April 1984 shows differences of 1 psu over a tidal cycle at 60-m depth, with spring-neap differences up to 1.2 psu, yet the difference between any two months can be as low as 0.4 psu. Though it is the best available, the sparseness of the interannual SJF forcing salinity data is the most likely limiting factor on the model's predictive abilities. Another complicating effect on SJF salinity is flow reversals of the SJF estuarine

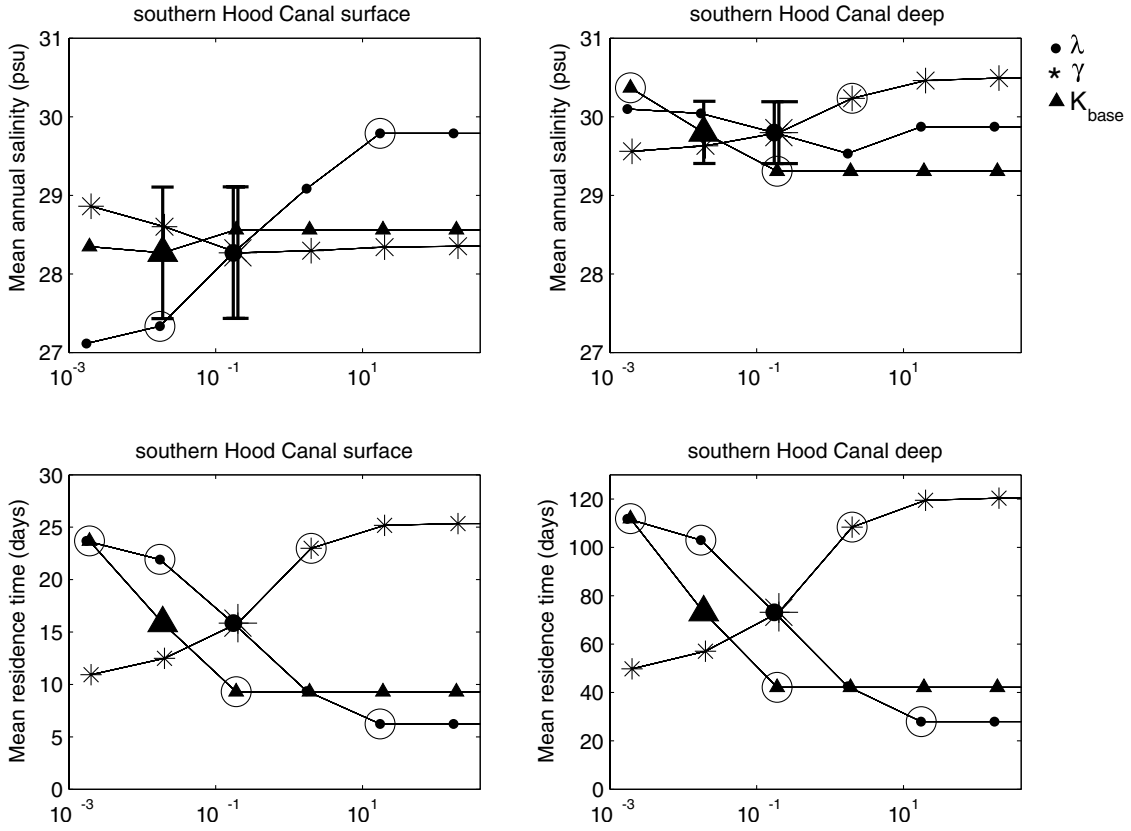

Fig. 6 Sensitivity of salinity (top two panels) and of residence time (bottom two panels) to calibration parameters. The bars mark the mean salinity plus or minus one standard deviation at the calibrated parameter value. The circles mark the first instance for each parameter that falls outside of the range of the bars. When the symbols are larger, that marks the calibrated value. Examples shown are for southern Hood Canal surface (left two panels) and deep (right two panels).

circulation associated with offshore storms (Cannon et al., 1990; Hickey et al., 1991). They have been observed to extend the full length of the SJF and to freshen the incoming deep water to Puget Sound. They occur on an event timescale which is not resolved by the salinity forcing dataset. The relative sparseness of the internal salinity data for interannual comparisons has the same aliasing problems as in the SJF salinity forcing. Available current meter mooring measurements indicate that the extent of the tidal effect on salinity varies by basin as well as by depth, but has a smaller effect within Puget Sound than in the SJF (Cannon et al., 1990; King County Dept. of Natural Resources, 1998).

The model's ability to hindcast interannual salinity variations was tested against twenty model runs with forcing years rearranged in random order. For all boxes, the Student-t test shows that r^2 values for the model with correctly ordered forcing are significantly higher than r^2 values for the ensemble of misordered forcing runs. This indicates that the model does have skill in hindcasting interannual variations. That misordered forcing runs have boxes with significant r^2 agreement indicates that the presence of a seasonal cycle can account for an important part of the correlation.

The model's ability to predict interannual variability, and thus to address questions of climate variability including the effects of the El Niño Southern Oscillation (ENSO) or the Pacific Decadal Oscillation (PDO), is limited by the resolution and availability of long-term SJF salinity forcing data. A major discrepancy in the salinity fit of the interannual model is the underestimation of the winter 1997 freshening in all basins. This is likely due to the four-month data gap (marked on Fig. 4b) during that winter, the period when SJF salinity usually is at its freshest. The following autumn was the beginning of a strong El Niño period, marked by anomalous freshening, an event the model does not capture. Some of the worst model agreement occurs before El Niño effects would be expected and most basins did recover agreement by late 1997. We thus cannot judge the model's ability to simulate this El Niño event because the preconditioning may have been missed. Currently, the forcing data record is sufficient for investigating seasonal variability, limited for interannual variability, and not complete enough to address questions about the effects of longer term climate oscillations or changes on circulation.

The calibration sensitivity tests indicate which boxes are sensitive to which parameters; examples are shown in Fig. 6. The calibrated values for the three mixing parameters each fall in the "salinity-sensitivity" range between the two asymptotic states for high and low mixing. If there were more mixing,

TABLE 3. Residence times by box, bounds determined by the calibration uncertainty, range of interannual values and years those extrema occurred.

Residence time (days)	mean	lower bound	upper bound	min annual	year	max annual	year
Admiralty							
surface	11.7	10.6	13.4	9.8	1996	17.9	1994
deep	15.9	13.1	16.6	13.4	1996	23.5	2001
Main							
surface	21.6	9.4	26.8	13.8	1994	28.1	1997
deep	37.8	15.2	46.1	23.4	1996	54.9	1997
South Sound							
surface	23.8	18.1	24.4	19.5	1996	32.6	2001
deep	23.0	17.4	23.7	18.9	1996	31.6	2001
Whidbey							
surface	4.9	2.5	6.5	4.3	1996	5.7	2001
deep	35.7	17.9	49.4	31.2	1996	41.7	2001
northern Hood							
surface	8.4	4.4	9.1	7.3	1996	19.5	2001
deep	14.6	7.6	15.8	10.5	1995	17.9	2001
southern Hood							
surface	15.8	9.3	22.0	11.9	1996	37.4	2001
deep	72.9	42.1	103.1	52.4	1996	99.0	2001
Narrows							
surface	1.2	n/a	n/a	0.9	1996	1.6	2001
deep	0.7	n/a	n/a	0.6	1996	1.0	2001

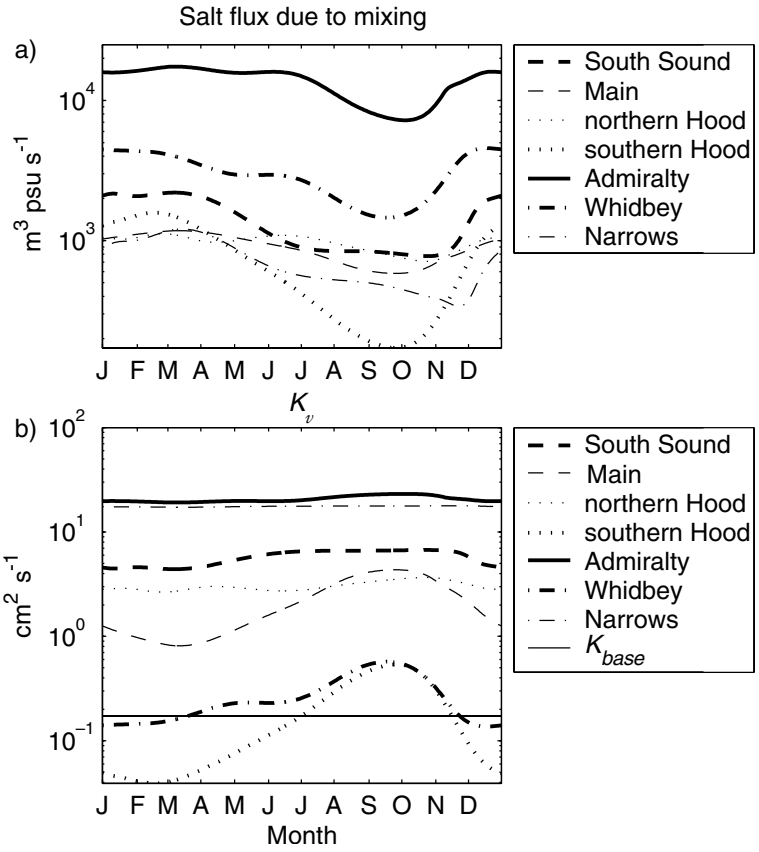

Fig. 7 (a) Salt flux due to mixing and (b) eddy diffusivity.

residence times would be shorter, and vice versa. In the top two panels of Fig. 6, the circled markers are the ones which fall outside the salinity range. Since these parameter values are globally constrained, the most restrictive values are then used as bounds for the range of residence times for all boxes, shown in the bottom two panels for southern Hood Canal. The

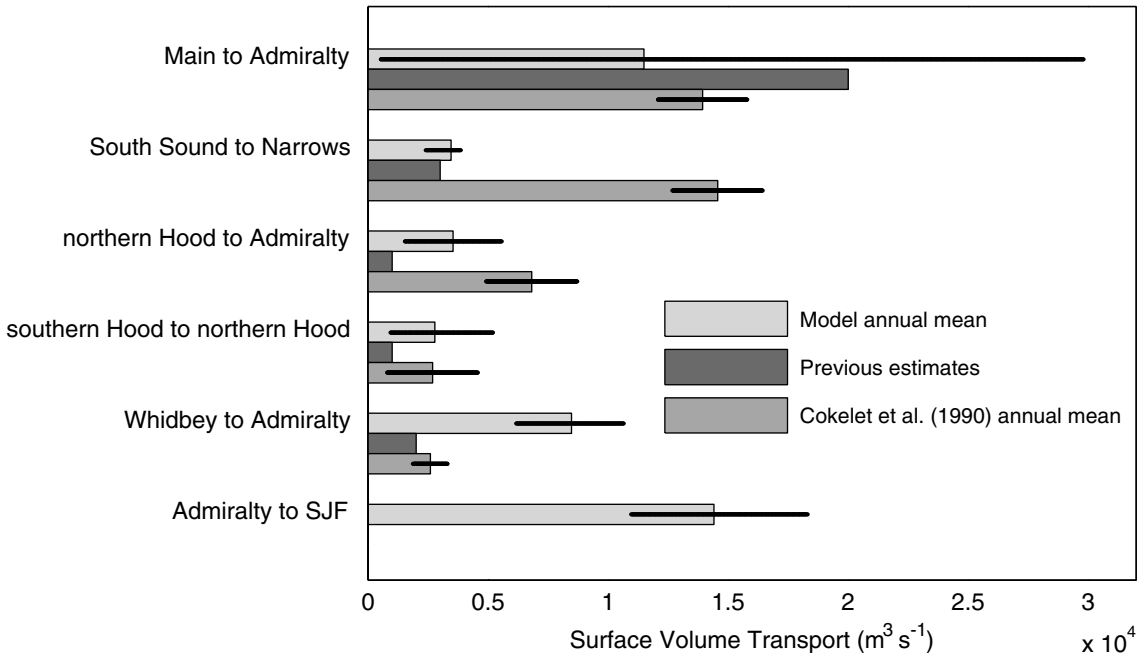

Fig. 8 Mean annual surface volume transports from the composite seasonal run: the bars on the model annual mean represent the maximum and minimum of monthly average volume transports. The bars on the Cokelet et al. (1990) annual mean are their error estimates.

parameter limits are: λ between 1.9×10^{-3} and 1.9×10^{-1}, γ below 2.0 and $K_{base}e$ between 1.5×10^{-2} and 15. These same limits occur in several other boxes, in addition to the example of southern Hood Canal. In the bottom two panels, which show sensitivity in terms of residence time, these limiting parameter values are again circled. The most constraining of these was then chosen as the bound: K_{base} for the upper bound and λ for the lower bound, for both boxes of the southern Hood Canal example. Table 3 includes columns for the upper and lower bounds on residence time for each box, found using this method. Most boxes are relatively tightly constrained, with Main and Whidbey basins and southern Hood Canal less so, but still within a factor of three. The dependence on α (not shown) is linear and most sensitive in Whidbey and Main basins. The upper bound, outside of the mean plus one standard deviation, is $\alpha = 0.4$, which says that within our data limits, up to 40% of Skagit River water could be leaving through Deception Pass.

The vertical salt flux due to mixing and the eddy diffusivity are shown in Fig. 7. The majority of mixing is thought to occur in the sill regions (Cokelet and Stewart, 1985). Admiralty Inlet and the Narrows have the highest K_v values. This does not translate into a high salt flux for the Narrows, due to its small area; more mixing occurs within Main Basin because of the larger area. The high degree of stratification in Whidbey Basin leads to a high salt flux due to the strong vertical salinity gradient, despite its relatively low eddy diffusivity. The modelled K_v values are smaller than previous estimates of vertical eddy viscosity values, A_v, by as much as an order of magnitude, but eddy viscosities generally are smaller than eddy diffusivities (Hansen and Rattray, 1965), and the relationship between values is consistent. Inferring the vertical eddy viscosities from model/measurement comparisons, Lavelle et al. (1991) estimated A_v to be: 30 $cm^2\ s^{-1}$ in Main Basin, 390 $cm^2\ s^{-1}$ in the Narrows, 160 $cm^2\ s^{-1}$ in deep Admiralty Inlet, and 80 $cm^2\ s^{-1}$ at the surface, whereas we find average values of 2.2 $cm^2\ s^{-1}$ for Main Basin, 17.6 $cm^2\ s^{-1}$ for the Narrows and 20.7 $cm^2\ s^{-1}$ for Admiralty Inlet. Microstructure turbulence measurements indicate that, volume-weighted, a comparable amount of mixing may occur in Main Basin shear zones as in sill regions, with measured diapycnal diffusivities ranging from 1.8 to 68 $cm^2\ s^{-1}$ (Mickett et al., 2004), so our average values are comparable to the low end of that range.

b *Transports and Residence Times*

Annual mean transports (Fig. 8) are smallest to and from southern Hood Canal and largest between Admiralty Inlet and the SJF. We show only surface box transports since deep box transports follow surface ones closely because throughflow from river discharge is small compared with the exchange circulation. To compare model transports to those based on observational data, we use previous transport estimates calculated from either current meter moorings or oxygen utilization compiled by Ebbesmeyer et al. (1984). The range of monthly average model transports span previous estimates in all basins except between Whidbey Basin and Admiralty Inlet and between northern Hood Canal and Admiralty Inlet, where the model predicts larger flows. Modelled transport in Deception Pass has an annual average of 1,137 $m^3\ s^{-1}$, which is quite

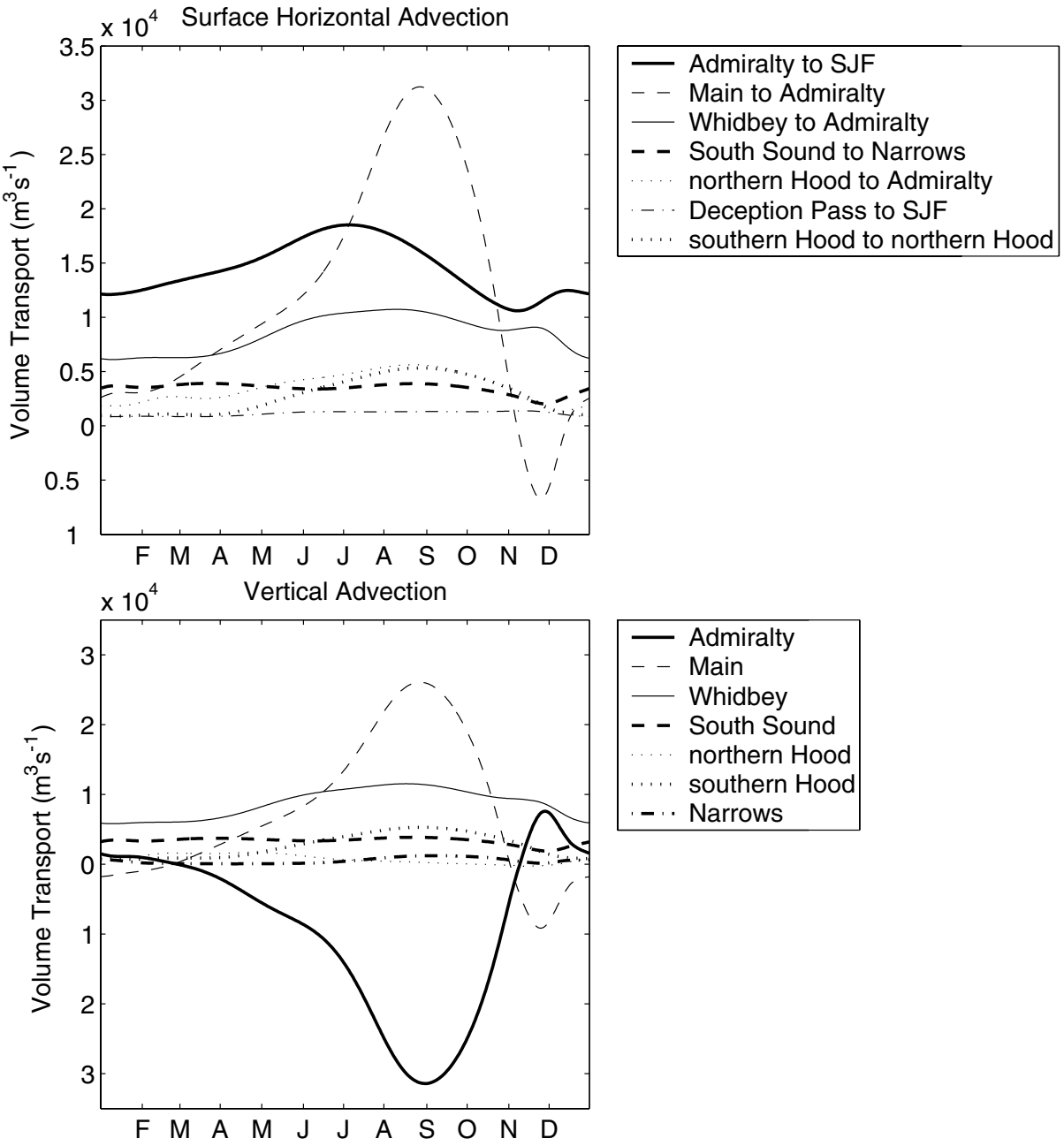

Fig. 9 Composite seasonal surface volume transports. Deep box transports mostly mirror surface transports. For horizontal transport, seaward is positive, for vertical transport, positive is from the deep box to the surface box.

close to the Collias et al. (1973) estimate of 1,125 $m^3 s^{-1}$ from eight days of current meter observations.

The degree of seasonal transport variation differs by basin, with transport maxima between 1.7 and 6 times the minima depending on the basin (Fig. 9). The largest seasonal variability is seen in the transport between Main Basin and Admiralty Inlet. It peaks in the late summer before dropping sharply in autumn, until it reverses direction. Main Basin vertical advection, normally upward, also reverses direction at this time, while Admiralty Inlet vertical advection, generally downward, reverses to upward. The seasonal flow reversals between Main Basin and Admiralty Inlet occur every year of the interannual run. The peak shape, amplitude, timing and even number of seasonal peaks is highly variable between years. It occurs throughout the acceptable ranges of tunable parameters in the calibration sensitivity study.

This transport drop is due to the increase in river flow into Whidbey Basin. When this fresh water enters Admiralty Inlet, it decreases the seaward salinity gradient between Admiralty Inlet and Main Basin, which determines the exchange circulation

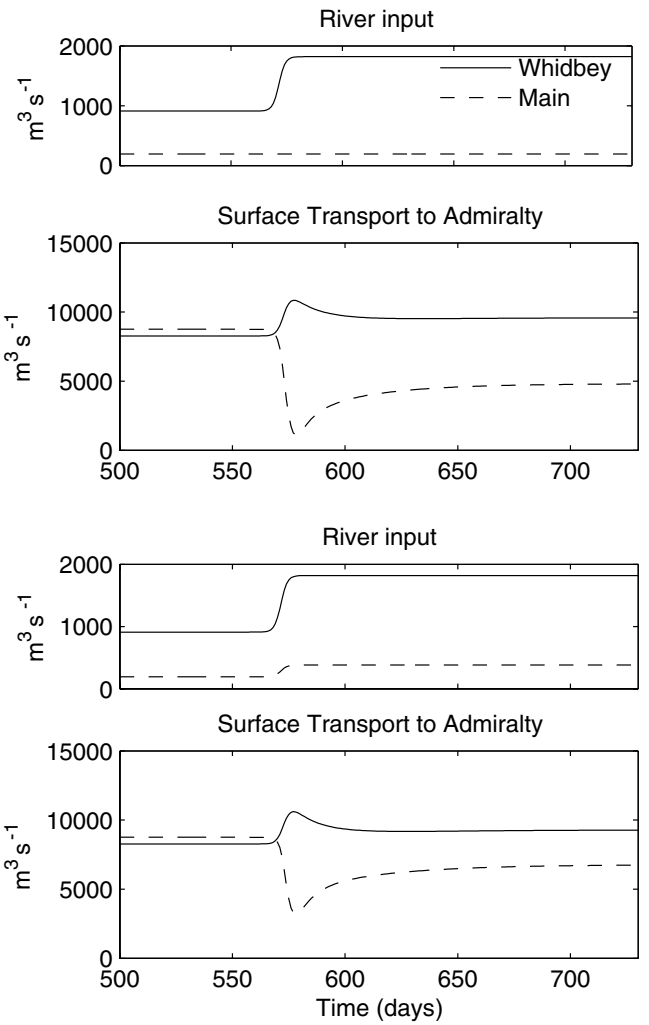

Fig. 10 Idealized test of effect of Whidbey Basin river flow on transport between Main Basin and Admiralty Inlet. The top two panels show the effect of doubling Whidbey river flow while Main Basin river flow is kept constant. The bottom two panels show the effect of doubling both river flows.

between the two basins. So, while total transport into and out of the system increases as expected with river flow, the circulation into Main Basin is reduced. This effect may be partly an artefact of the model box configuration. The distribution of outflow water from the Whidbey Basin between Main Basin and Admiralty Inlet takes place in a complicated triple junction, whereas the model simplifies the outflow entering Admiralty Inlet in its entirety. This simplification is justified by a recent study of this junction that indicates that most of the Whidbey Basin surface water flows north upon reaching this region (Ebbesmeyer et al., 2001). That study indicates that the assumption of two-layer flow is violated in parts of this region and is likely a more significant simplification than the geometry chosen for the model.

Evidence for the Main Basin transport drop is seen in the data, with the decrease in the salinity gradient between the basins seen in the composite DoE data. Transports calculated

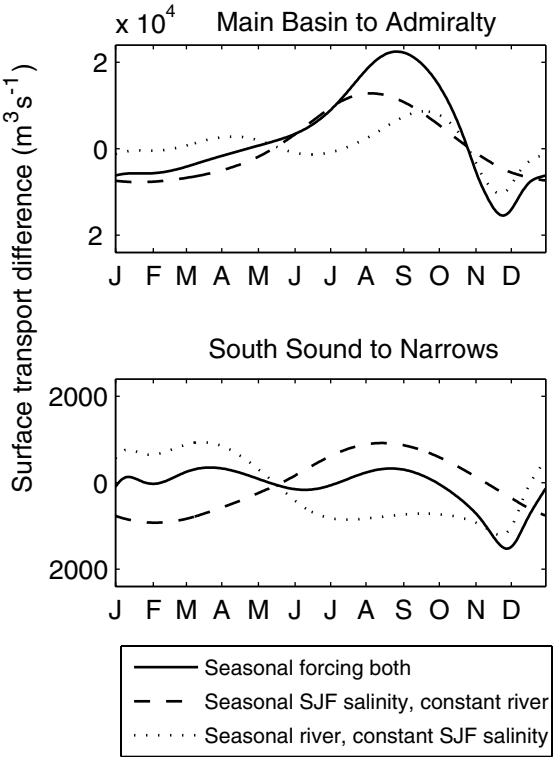

Fig. 11 Seasonal forcing sensitivity: only surface boxes are shown; deep transports closely mirror surface transports.

from historical current meter records, categorized by season of study, show the lowest transports occurring in the autumn (Ebbesmeyer et al., 1984). Previous current meter studies have discussed the effect of freshwater inflow reducing deep water intrusions into Admiralty Inlet (Geyer and Cannon, 1982; Cannon, 1983; Lavelle et al., 1991), which could reduce transport up the main stem of Puget Sound. The decreased autumn transport between Main Basin and Admiralty Inlet is a transient feature because the increase in Main Basin river flow soon partially restores the seaward salinity gradient. The same effect, though less pronounced, can also be seen in model transports between Admiralty Inlet and northern Hood Canal. A similar effect of transport reversal has been seen in the tributaries of Chesapeake Bay during the spring freshet from the Susquehanna River (Carter and Pritchard, 1988).

A simple test was performed for the response to a sharp jump in river flow while holding SJF salinity constant. In the first experiment, only the river flow into Whidbey Basin was doubled and in the second experiment, both Whidbey Basin and Main Basin river flows were doubled (Fig. 10). Both experiments show an initial, large decrease in transport between Main Basin and Admiralty Inlet, and subsequent relaxation to a new steady state, with an adjustment time of 25–30 days. This is comparable to the residence time in Main Basin. While some work has been done on the adjustment time for coastal plain estuaries (Kranenburg, 1986; MacCready, 1999; Hetland and Geyer, 2004), no theory exists for the adjustment time in complicated systems such as

Table 4. Root mean square of residual variance for each of the forcing sensitivity runs in $m^3\ s^{-1}$. The top two sections show seasonal forcing and the bottom two show interannual forcing

		Admiralty	Main	southern Sound	Whidbey	northern Hood	southern Hood	Narrows
Seasonal	Surface							
	total	2454	11001	484	1680	1368	1640	667
	river	1867	4304	749	545	408	461	949
	S_{SJF}	3100	7252	644	1535	1328	1406	1307
	Deep							
	total	2771	11124	495	2057	1422	1694	700
	river	1475	4380	689	671	433	515	888
	S_{SJF}	3267	7252	644	1709	1328	1406	1307
Interannual	Surface							
	total	4082	10602	977	1627	2412	1688	1452
	river	2620	4883	677	851	1724	1059	965
	S_{SJF}	2733	8399	644	1355	1312	1087	1082
	Deep							
	total	3941	10599	940	1709	2376	1667	1417
	river	2226	4874	621	713	1677	1024	909
	S_{SJF}	2872	8399	644	1501	1312	1087	1082

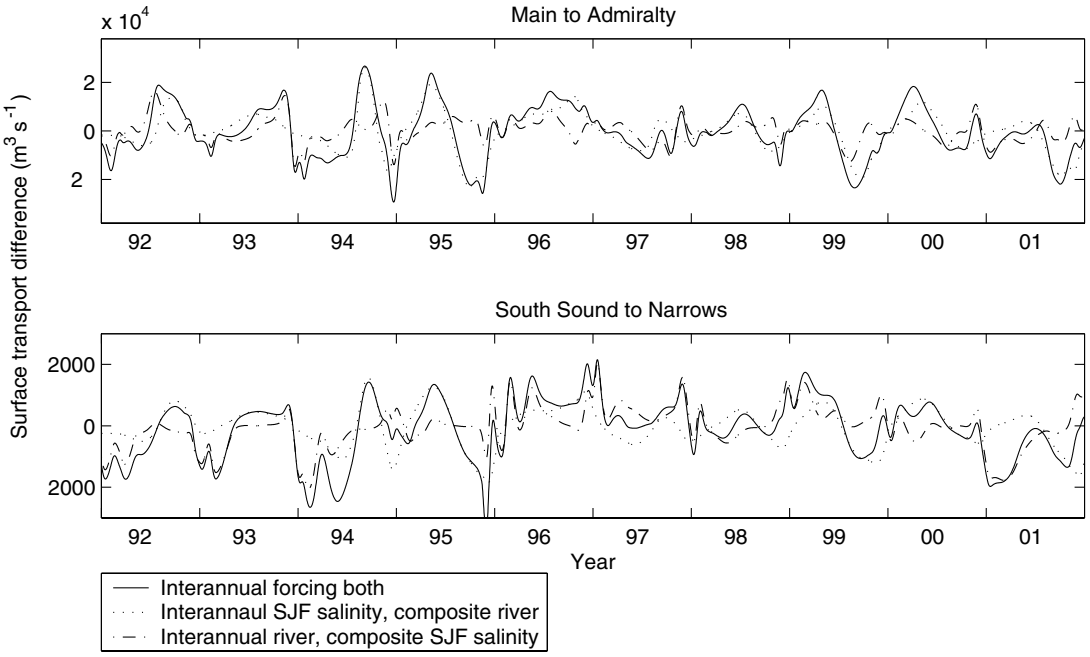

Fig. 12 Interannual forcing sensitivity: only surface boxes are shown, but deep transports closely mirror surface transports. A composite seasonal forcing run has been subtracted from each run in order to obtain the anomaly. Ticks mark the start of a year.

Puget Sound. The second case shows that, while Main Basin river inputs can mitigate this effect, they cannot overcome it as long as river flow changes are kept proportional.

Residence times can be calculated from transports by dividing the volume of a box by the sum of all volume fluxes into that box. First we look at the residence times calculated from annual average transports. Surface boxes and both Narrows boxes which have small volumes have especially short residence times. The regions with higher mixing, Admiralty Inlet, northern Hood Canal, the Narrows and South Sound all have relatively short residence times for both boxes (Table 3). The shorter residence time of the deep versus surface box in South Sound is due to the smaller volume. Deep Main and Whidbey basins have residence times greater than one month. The weak transport through southern Hood Canal means that its deep residence time is two and a half months.

If residence times are calculated from average transports over shorter intervals, they vary extensively. Winter transports lead to residence time estimates exceeding 250 days for southern Hood Canal when the high river flow leads to high stratification, while late summer estimates are as short as 40 days. Estimates are also highly variable between years. Average annual residence times from the interannual run vary by a factor of two in the surface Hood Canal boxes between years, and deep southern

Hood Canal varies between years from a minimum residence time of 52 days to a maximum of 99 days (Table 3).

When comparing model residence times to previous estimates compiled by Ebbesmeyer et al. (1984), it is necessary to combine surface and deep boxes and to compare the range of monthly average model results. While some of the estimates based on currents were from historical compilations encompassing a wider time period, most were from mid-channel deployments of current meters lasting from a few days to two months. The generally better agreement of the range of this model's results with data estimates than the Cokelet et al. (1990) mean annual transports is likely due to the timescale differences. For the basins where model transport ranges do not span the previous estimates, the Cokelet et al. (1990) model comes closer to the data estimates for Whidbey Basin to Admiralty Inlet transport, but this model comes close for northern Hood Canal to Admiralty Inlet.

The 48.8 day average residence time in Main Basin is longer than the previous estimate of 30 days, 46.1 days for South Sound is close to the previous estimate of 57 days, while the estimates of 37.2 days for Whidbey Basin and 85.5 days for southern Hood Canal are much shorter than the previous estimates of 162 and 279 days respectively. The high degree of both seasonal and interannual transport variability shown in this study indicates that it is not necessarily relevant to compare residence times during different years, during different time periods. Shorter residence times in these highly productive regions mean that nutrients and oxygen are replenished more often than previously thought.

The wide range in residence times between years in Main Basin is partly due to variability in the fall flow reversal. The year with the shortest residence times in most of the basins, 1996, has the smallest flow reversal between Main Basin and Admiralty Inlet. Since residence times are calculated based on annual average transports, a flow reversal reduces the transport, which in turn increases the residence time. The occurrence and duration of reversals thus play a large part in this calculation of residence time, which may not accurately represent the time a parcel of water spends in a particular basin. The reversals in the model are likely an indication of a period of time when the assumption of two-layer flow is insufficient. Under these conditions it is more likely for a three-layer flow to develop than a complete reversal.

c *Sensitivity to Forcing Mechanism*

The tests of relative importance of river versus SJF salinity forcing mechanism on the seasonal transport cycle show that both mechanisms affect transport in all of the boxes. Figure 11 shows two examples of comparisons between forcing mechanisms: surface Main Basin to Admiralty Inlet where SJF salinity forcing has a larger net effect, and South Sound to the Narrows where river forcing has a slightly larger net effect. In most basins, the run with composite forcing for both mechanisms follows the composite SJF salinity forcing run more closely, but is modulated by the river forcing. The r.m.s values of the time series for each box, shown in Table 4, show that, of the total seasonal variance, SJF salinity variability has a larger effect than river variability in all basins except South Sound. The dominance of river forcing in South Sound is likely due to the mixing in the Narrows reducing the ability of the SJF salinity signal to propagate past there. This sensitivity study enables us to see that the sharp drop in Main Basin to Admiralty Inlet transport in the fall is due to river forcing. There is only a gradual decrease when the model is forced by constant river flow and seasonally varying SJF salinity.

Interannual variability has as large an effect on transports as seasonal variability, as exhibited by the similarity between seasonal and interannual r.m.s. values of total variability. For the tests of interannual variability (Fig. 12), the same two examples used in the seasonal case are shown, with the same mechanism dominating each. Looking at Table 4, river variability now has a larger net effect on the r.m.s. of transport variability in four more boxes. There is no clear pattern of a dominant mechanism based on proximity to the SJF or river input.

4 Conclusions

This box model of Puget Sound circulation represents advances over previous modelling efforts because it is time dependent and prognostic, and covers Puget Sound in its entirety. The most noticeable seasonal feature is the autumn transport drop between Main Basin and Admiralty Inlet, following an increase of river flow into Whidbey Basin which is due to the seaward input of river flow decreasing the salinity gradient. This indicates the need to consider the effect of branching in hypotheses of estuarine circulation. Forcing sensitivity tests indicate that variability in both river forcing and external salinity forcing are important. Since the external salinity forcing data are undersampled and much of the previous work has focused on river forcing, there is a need for higher resolution, extended monitoring of ocean conditions. Interannual transport variations are of a similar magnitude to seasonal ones, which should be taken into account when planning sampling strategies. Estimates of residence times based on a year or less of data should be considered in the context of this variability.

Acknowledgements

The authors thank G. Cannon and two anonymous reviewers for comments and criticisms on this manuscript. We also thank J. Newton and the Washington State Department of Ecology and the U.S. Geological Survey for data provided via their web sites. The Lavelle et al. (1988) model used to compute u_T was converted for use in Matlab by Dave Winkel. This research was supported by the King County (WA) Department of Natural Resources and by the National Ocean Partnership Program.

References

BARNES, C.A. and E. E. COLLIAS. 1958. Some consideration of oxygen utilization rates in Puget Sound. *J. Mar. Res.* **17**:68–80.

BRETSCHNEIDER, D.E.; G.A. CANNON, J.R. HOLBROOK and D.J. PASHINSKI. 1985. Variability of subtidal current structure in a fjord estuary: Puget Sound,

Washington. *J. Geophys. Res.* **90**(C6):11,949–11,958.

CANNON, G.A. 1983. An overview of circulation in the Puget Sound estuarine system. NOAA Technical Memorandum. ERL PMEL-48, 30 pp.

—— and N.P. LAIRD. 1978. Variability of currents and water properties from year-long observations in a fjord estuary. In: *Hydrodynamics of Estuaries and Fjords*, C.J. Nihoul (Ed.), Elsevier, Amsterdam. pp. 515–535.

——; J.R. HOLBROOK and D.J. PASHINSKI. 1990. Variations in the onset of bottom water intrusions over the entrance sill of a fjord. *Estuaries,* **13**(1):31–42.

CARTER, H.H. and D.W. PRITCHARD. 1988. Oceanography of Chesapeake Bay. In: *Hydrodynamics of Estuaries*, B. Kvjerfve (Ed.), CRC Press, Boca Raton, Florida. pp. 1–16.

COKELET, E.D. and R.J. STEWART. 1985. Exchange of water in fjords: the efflux/reflux theory of advective reaches separated by mixing zones. *J. Geophys. Res.* **90**:7287–7306.

——; R.J. STEWART and C.C. EBBESMEYER. 1990. The annual mean transport in Puget Sound. NOAA Technical Memorandum, ERL-PMEL-92. 54 pp.

COLLIAS, E.; C.A.BARNES and J.A. LINCOLN. 1973. Skagit Bay study dynamical oceanography: final report. Dept. of Oceanography, University of Washington Ref M73-73. 186 pp.

——; N. MCGARY and C.A. BARNES. 1974. Atlas of physical and chemical properties of Puget Sound and its surrounding approaches. Dept. of Oceanography, University of Washington, WSG-74-1. 235 pp.

COX, J.M.; C.C. EBBESMEYER, C.A. COOMES, J.M. HELSETH, L.R.HINCHEY, G.A. CANNON and C.A. BARNES. 1984. Synthesis of current measurements of Puget Sound, Washington – Volume I: Index of current measurements made in Puget Sound from 1908–1980 with daily and record averages for selected measurements. NOAA Technical Memorandum, NOS OMS 3. 38 pp.

DYER, K.R. 1997. *Estuaries: A physical introduction.* 2nd Edition. John Wiley annd Sons, Chichester, New York. 195 pp.

EBBESMEYER, C.C. and C.A. BARNES. 1980. Control of a fjord basin's dynamics by tidal mixing in embracing sill zones. *Estuar. Coastal Mar. Sci.* **11**(3):311–330.

——; C.A. COOMES, J.M. COX, J.M. HELSETH, L.R. HINCHEY, G.A. CANNON and C.A. BARNES. 1984. Synthesis of current measurements in Puget Sound, Washington – Volume 3: Circulation in Puget Sound: An interpretation based on historical records of currents. NOAA Technical Memorandum. NOS OMS 5. 73 pp.

——; ——, G.A. CANNON and D.E. BRETSCHNEIDER. 1989. Linkage of ocean and fjord dynamics at decadal period. In: *Aspects of Climate Variability in the Pacific and Western Americas: Geophysical Monograph 55.* D.H. Peterson (Ed.) American Geophysical Union, Washington, D.C. pp. 399–417.

——; G.A. CANNON, B.J. NAIRN, M. KAWASE and W.P. FOX. 2001. Puget Sound physical oceanography related to the triple junction region. Interim Report for King County Department of Natural Resources, 4 September 2001. 148 pp.

EDWARDS, K. A.; P. MACCREADY, J. N. MOUM, G. PAWLAK, J. KLYMAK and A. PERLIN. 2004. Form drag and mixing due to tidal flow past a sharp point. *J. Phys. Oceanogr.* **34**:1297–1312.

FRIEBERTSHAUSER, M.A. and A.C. DUXBURY. 1972. A water budget study of Puget Sound and its subregions. *Limnol. Oceanogr.* **17**:237–247.

GEYER, W.R. and G.A. CANNON. 1982. Sill processes related to deep water renewal in a fjord. *J. Geophys. Res.* **87**(C10):7985–7996.

——; J.H. TROWBRIDGE and M.M. BOWEN. 2000. The dynamics of a partially mixed estuary. *J. Phys. Oceanogr.* **30**:2035–2048.

HAGY, J.D.; L.P. SANFORD and W.R. BOYNTON. 2000. Estimation of net physical transport and hydraulic residence times for a coastal plain estuary using box models. *Estuaries,* **23**(3):328–340.

HAMILTON, P.; J.T. GUNN AND G.A. CANNON. 1985. A box model of Puget Sound. *Estuar. Coastal Shelf Sci.* **20**:673–692.

HANSEN, D.V. and M. RATTRAY. 1965. Gravitational circulation in straits and estuaries. *J. Mar. Res.* **23**:104–122.

HETLAND, R.D. and W.R. GEYER. 2004. An idealized study of long, partially mixed estuaries. *J. Phys. Oceanogr.* **34**(12):2677–2691.

HICKEY, B.M. 1989. Patterns and processes of circulation over the Washington continental shelf and slope. In: *Coastal Oceanography of Washington and Oregon*, M.R. Landry and B.M. Hickey (Eds), Elsevier, Amsterdam, pp. 41–115

——; R.E. THOMSON, H. YIH and P.H. LEBLOND. 1991. Velocity and temperature fluctuations in a buoyancy-driven current off Vancouver Island. *J. Geophys. Res.* **96**(C6):10507–10538.

HOLBROOK, J.R.; R.D. MUENCH, D.G. KACHEL and C. WRIGHT. 1980. Circulation in the Strait of Juan de Fuca: Recent oceanographic observations in the Eastern Basin. NOAA Technical Report, ERL-PMEL 33, 42 pp.

KING COUNTY DEPT. OF NATURAL RESOURCES. 1998. Water Quality Status Report for Marine Waters, Seattle, WA. 98 pp.

——. 2002. Brightwater Marine Outfall: Puget Sound Marine Modeling Report. 45 pp.

KRANENBURG, C. 1986. A timescale for long-term salt intrusion in well-mixed estuaries. *J. Phys. Oceanogr.* **16**:1329–1331.

LAVELLE, J.W.; H.O. MOFJELD, E. LEMPRIERE-DOGGETT, G.A. CANNON, D.J. PASHINSKI, E.D. COKELET, L. LYTLE and S. GILL. 1988. A multiple connected channel model of tides and tidal currents in Puget Sound, Washington and a comparison with updated observations. NOAA Technical Memorandum, ERL PMEL-84. 108 pp.

——; E.D. COKELET and G.A. CANNON. 1991. A model study of density intrusions into and circulation within a deep, silled estuary: Puget Sound. *J. Geophys. Res.* **96**(C9):16,779–16,800.

LEWIS, R.E. 1996. Relative contributions of interfacial and bed generated mixing to the estuarine energy balance. In: *Mixing in Estuaries and Coastal Seas*, C. Pattiaratchi (Ed.), Coastal and Estuarine Studies Series, American Geophysical Union, Vol. 50 pp. 250–266.

LI, M.; A. GARGETT and K. DENMAN. 1999. Seasonal and interannual variability of estuarine circulation in a box model of the Strait of Georgia and Juan de Fuca Strait. ATMOSPHERE-OCEAN, **37**(1):1–19.

LINCOLN, J.H. 1977. Derivation of freshwater inflow into Puget Sound. University of Washington Department of Oceanography Special Report No. 72. University of Washington, Seattle, Washington. 20 pp.

MACCREADY, P. 1999. Estuarine adjustment to changes in river flow and tidal mixing. *J. Phys. Oceanogr.* **29**: 708–726.

MICKETT, J.B.; M. C. GREGG and H.E. SEIM. 2004. Direct measurement of diapycnal mixing in a fjord reach – Puget Sound's Main Basin. *Estuar. Coastal Shelf Sci.* **59**: 539–558.

MONISMITH, S.G. and D.A. FONG. 1996. A simple model of mixing in stratified tidal flows. *J. Geophys. Res.* **101**: 28,583–28,595.

MUNK, W. H. and E. R. ANDERSON. 1948. Notes on the theory of the thermocline. *J. Mar. Res.* **3**: 276–295.

NAIRN, B.J. and M. KAWASE. 2002. Comparison of observed circulation patterns and numerical model predictions in Puget Sound, WA. *In:* Proc. 2001 Puget Sound Research Conference. T. Droscher (Ed.), Puget Sound Water Quality Action Team. Olympia, Washington. 9 pp.

PRITCHARD, D. W. 1954. A study of the salt balance in a coastal plain estuary. *J. Mar. Res.* **13**:133–144.